LIMK-Dependent Actin Polymerization in Primary Sensory Neurons Promotes the Development of Inflammatory Heat Hyperalgesia in Rats

Yi Li, Fang Hu, Hai-Jing Chen, Yi-Juan Du, Zhi-Ying Xie, Ying Zhang, Jun Wang and Yun Wang (June 24, 2014)

Science Signaling **7** (331), ra61. [doi: 10.1126/scisignal.2005353]

NEUROSCIENCE

LIMK-Dependent Actin Polymerization in Primary Sensory Neurons Promotes the Development of Inflammatory Heat Hyperalgesia in Rats

Yi Li,[1]* Fang Hu,[1]* Hai-Jing Chen,[1]* Yi-Juan Du,[1] Zhi-Ying Xie,[2] Ying Zhang,[1] Jun Wang,[3]† Yun Wang[1,4]†

Changes in the actin cytoskeleton in neurons are associated with synaptic plasticity and may also be involved in mechanisms of nociception. We found that the LIM motif–containing protein kinases (LIMKs), which regulate actin dynamics, promoted the development of inflammatory hyperalgesia (excessive sensitivity to painful stimuli). Pain is sensed by the primary sensory neurons of dorsal root ganglion (DRG). In rats injected with complete Freund's adjuvant (CFA), which induces inflammatory heat hyperalgesia, DRG neurons showed an increase in LIMK activity and in the phosphorylation and thus inhibition of the LIMK substrate cofilin, an actin-severing protein. Manipulations that reduced LIMK activity or abundance, prevented the phosphorylation of cofilin, or disrupted actin filaments in DRG neurons attenuated CFA-induced heat hyperalgesia. Inflammatory stimuli stimulated actin polymerization and enhanced the response of the cation channel TRPV1 (transient receptor potential V1) to capsaicin in DRG neurons, effects that were reversed by the knockdown of LIMK or preventing cofilin phosphorylation. Furthermore, inflammatory stimuli caused the serine phosphorylation of TRPV1, which was abolished by preventing cofilin phosphorylation in DRG neurons. We conclude that LIMK-dependent actin rearrangement in primary sensory neurons, leading to altered TRPV1 sensitivity, is involved in the development of inflammatory hyperalgesia.

INTRODUCTION

The cytoskeleton is an intricate, fibrous subcellular network that contains microtubules, microfilaments and intermediate filaments, and their associated proteins (*1*). Dynamic and differential changes that cause cytoskeletal rearrangement occur during different cellular processes according to the cell type and the specific function of the cell. For example, reorganization of the cytoskeleton occurs during axogenesis and neurite formation in neurons (*2*–*4*). In rats, the disruption of microfilaments substantially attenuates hyperalgesia caused by the injection of epinephrine or its downstream mediators into paws (*5*). Therefore, the cytoskeleton is a critical regulator in inflammatory pain plasticity (*6*).

The modulation of neuronal actin may be involved in the cytoskeletal changes that are associated with synaptic plasticity at pre- and postsynaptic terminals (*7*) and may contribute to the mechanisms of nociception. LIM motif–containing protein kinase (LIMK), a key regulator of actin dynamics, is a protein kinase family that consists of only two members: LIMK1 and LIMK2 (*8*–*10*). LIMKs play an important role in translating signals from the guanosine triphosphatase (GTPase) Rho into biological effects. Phosphorylation of the conserved threonine residues, Thr^{508} and Thr^{505}, in the activation loop results in the activation of LIMK1 and LIMK2. LIMK can be activated by several kinases that act downstream of Rho GTPase: Pak1, Pak2, Pak4 (p21-activated kinases 1, 2, and 4), ROCK I and II (Rho-associated kinases I and II), and MRCKα (myotonic dystrophy kinase-related Cdc42-binding kinase α) (*11*–*19*).

In contrast to other kinases that have multiple substrates, the only known substrate of LIMK is the actin-depolymerizing factor (ADF) cofilin (*20*, *21*). LIMK regulates actin polymerization by phosphorylating and thus inactivating cofilin, thereby contributing to diverse cellular functions such as cell motility, morphogenesis, division, differentiation, apoptosis, neurite extension, and oncogenesis (*22*–*26*).

LIMK1 mRNA is predominantly expressed in neural tissues, particularly in the dorsal root ganglion (DRG), which is the primary nociceptor, and the spinal cord, which can receive the pain signaling from DRG and conduct it to brain; LIMK2 mRNA is also expressed in neural tissue (*27*, *28*). Neural plasticity is involved in the generation of pain hypersensitivity. $LIMK1^{-/-}$ mice have abnormal dendritic spine morphology and synaptic function. $LIMK1/2^{-/-}$ mice exhibit much more severe abnormalities in synaptic function (*29*–*31*). Inhibiting the phosphorylation of cofilin in the granule cells of the dentate gyrus partially impairs the late phase of long-term potentiation (*32*). Additionally, the neurotrophin nerve growth factor (NGF) plays a major role in the production of inflammatory hyperalgesia (*33*, *34*). Because NGF stimulates the activity of both LIMK1 and LIMK2 in PC12 cells (*25*), these data suggest that the LIMK-cofilin-microfilament pathway may contribute to inflammation- or nerve injury–induced pain hypersensitivity. Here, we found that LIMK1 and LIMK2 participate in the development of complete Freund's adjuvant (CFA)–induced inflammatory pain. Many protein kinases that are involved in pain sensitivity, such as PKA [adenosine 3′,5′-monophosphate (cAMP)–dependent protein kinase], PKCε (protein kinase Cε), and ERK1/2 (extracellular signal–regulated kinase 1/2), can bind to cytoskeletal elements (*35*–*40*). Inflammatory mediators often activate these protein kinases through their cognate receptors, leading to the phosphorylation of the cation channel TRPV1

[1]Neuroscience Research Institute and Department of Neurobiology, Key Laboratory for Neuroscience of Ministry of Education and Health, School of Basic Medical Sciences, Peking University, Beijing 100191, China. [2]Beijing Huijia Private School, Beijing 102200, China. [3]Department of Anatomy and Histology, School of Basic Medical Sciences, Peking University, Beijing 100191, China. [4]PKU-IDG/McGovern Institute for Brain Research, Peking University, Beijing 100871, China.
*These authors contributed equally to this work.
†Corresponding author. E-mail: wangy66@bjmu.edu.cn (Y.W.); wangjun74008@bjmu.edu.cn (J.W.)

(transient receptor potential V1) and rapid and dynamic changes in pain sensitivity (*41*–*45*). Here, we also found that phosphorylation by kinases linked to CFA-induced signaling enhances the function of the TRPV1 channel and that F-actin (filamentous actin) regulated by LIMK may function as a scaffold.

RESULTS

LIMK1 and LIMK2 are rapidly activated in primary sensory neurons after CFA-induced inflammatory pain hypersensitivity

Western blotting revealed high abundance of LIMK1 and LIMK2 in the DRG and spinal dorsal horn (Fig. 1A). However, in vitro kinase assays showed that the kinase activity was higher in the DRG than in the spinal dorsal horn (Fig. 1B). Thus, we focused on the functions of LIMK1 and LIMK2 in primary sensory neurons.

To determine whether peripheral noxious stimuli induce a change in the protein abundance and activity patterns of LIMK1 and LIMK2 in the DRG, we used a model of inflammatory pain induced by CFA injection (*46*). CFA was injected into the plantar surface of the rats' left hindpaws. The injection caused localized inflammation associated with swelling and erythema. Heat hyperalgesia was evoked 0.5 hour after the injection and was maintained for more than 1 week in the ipsilateral paw.

We evaluated the kinase activity of LIMK1 in the ipsilateral lumbar vertebrae 4 to 6 (L4-L6) DRG with an in vitro kinase assay. LIMK1 activity was relatively low in nontreated rats, but increased after CFA injection, peaking at 1 hour, and remained high for up to 1 day after CFA injection. His_6-cofilin protein, the abundance of which was determined by Coomassie blue staining, was used as a loading control (Fig. 1C). LIMK1 activity was increased about threefold 1 hour after CFA injection (Fig. 1C). Western blotting revealed that LIMK1 protein abundance did not change in the ipsilateral DRG after CFA treatment (Fig. 1D). LIMK2 activity increased after the CFA injection, peaking at 0.5 hour, and then declined to basal

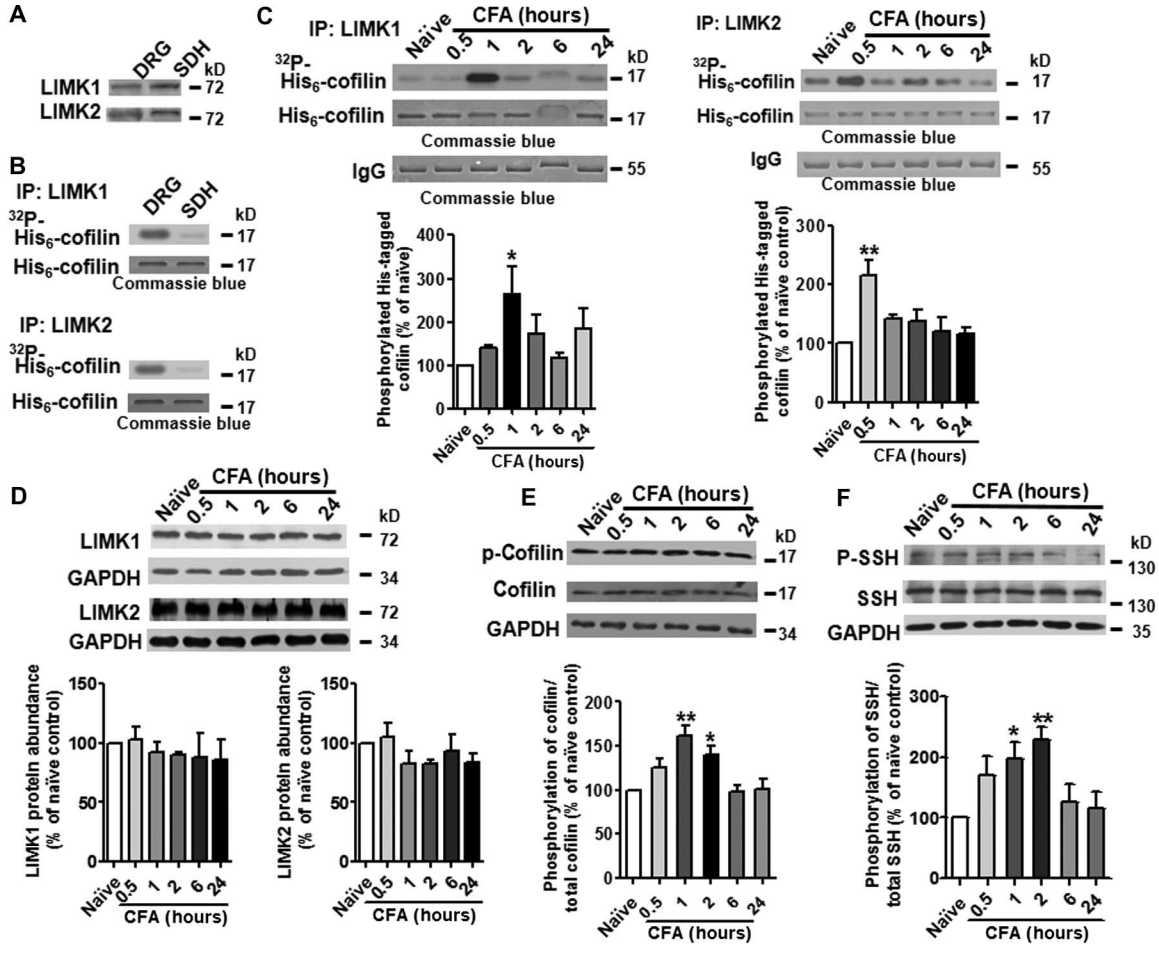

Fig. 1. LIMK1 and LIMK2 abundance and activity under normal physiological or inflammatory conditions. (**A** and **B**) Representative Western blots of LIMK (A) and in vitro kinase assays of LIMK activity (B) in the DRG and spinal dorsal horn (SDH) in naïve rats. (**C** and **D**) Time course of LIMK kinase activity (C) and LIMK protein abundance (D) from 0.5 hour to 1 day after CFA injection (n = 3 independent experiments). (**E** and **F**) Representative Western blots of phosphorylated and total cofilin (E) and SSH1L (F) in rat DRG from 0.5 hour to 1 day after CFA injection. Quantification of the phosphorylated signal used the density ratio of phosphorylated protein to total protein (n = 3 independent experiments). In vitro kinase assays used purified His_6-cofilin as a substrate, and inputs were analyzed by Coomassie blue staining. Graphs show means ± SEM. The data were analyzed by analysis of variance (ANOVA) followed by Dunnett's multiple comparison test (*P < 0.05, **P < 0.01, compared with the naïve control).

amounts between 1 hour and 1 day (Fig. 1C). LIMK2 protein abundance did not change during this process (Fig. 1D). The sequential increases in LIMK2 and LIMK1 activation might be due to distinct Rho family GTPases. LIMK1 is activated by Rac1 and Cdc42, but not RhoA, whereas LIMK2 is activated by RhoA and Cdc42, but not Rac1 (*11*, *16*, *21*, *47*).

As previously reported, the major function of LIMK1 and LIMK2 is to phosphorylate cofilin at Ser^3, which results in its inactivation (*25*). CFA injection induced the activation of LIMK1 and LIMK2 (Fig. 1C). As expected, Western blotting and quantitative analyses showed that phosphorylation of Ser^3 in cofilin significantly increased 1 hour after CFA injection and did not decrease to baseline until 2 hours after the CFA injection (Fig. 1E). Cofilin is inactivated by LIMK-mediated phosphorylation and is reactivated by the phosphatase Slingshot (SSH), mainly by the SSH1L isoform (*23*, *48*–*50*). We found that the phosphorylation of Ser^{978} in SSH1L, which inactivates the phosphatase so that it cannot dephosphorylate phosphorylated cofilin (*48*), was increased after CFA injection (Fig. 1F). Together, these results suggest that the activation of LIMK1 and LIMK2 and the inactivation of SSH1L after CFA injection inactivate cofilin.

Overexpression of dominant-negative mutants of LIMK attenuated heat hyperalgesia induced by CFA injection

The activation of LIMK and increased phosphorylation of cofilin after CFA injection suggest that LIMK might play a role in pain transmission. Thus, we further investigated whether LIMK activation in the early stages of CFA-induced inflammation contributed to the induction of pain hypersensitivity. Because phosphorylation of the conserved threonine residues, Thr^{508} and Thr^{505}, in the activation loop results in the activation of LIMK1 and LIMK2 and changing Thr^{508} or Thr^{505} to valine in the kinase domain of LIMK1 and LIMK2 abrogates their activity (*11*, *16*, *17*), we constructed wild-type LIMK1 and LIMK2 constructs (pEGFP-LIMK1 and pEGFP-LIMK2) and dominant-negative LIMK1 and LIMK2 constructs (pEGFP-T508V-LIMK1 and pEGFP-T505V-LIMK2, in which threonine residues were mutated to valines).

We measured paw withdrawal latency in rats that had been injected intrathecally with wild-type or dominant-negative LIMK or EGFP (enhanced green fluorescent protein) constructs. Basal nociceptive responses were not affected (Fig. 2A). In response to CFA injection, rats overexpressing T508V-LIMK1 showed substantially increased withdrawal latency of the ipsilateral paw compared with rats overexpressing EGFP or wild-type LIMK (Fig. 2A). The area under the curve of the time course showed that compared with rats overexpressing EGFP, those overexpressing the dominant-negative T508V-LIMK1 showed significantly reduced CFA-induced heat hyperalgesia (Fig. 2B). Rats overexpressing wild-type LIMK1 or EGFP showed similar paw withdrawal latencies (Fig. 2, A and B). In vitro kinase assays indicated that LIMK1 activity in the DRG was inhibited by the overexpression of T508V-LIMK1, but not by that of EGFP (Fig. 2C). The phosphorylation of cofilin decreased in the ipsilateral DRG as a result of the overexpression of T508V-LIMK1 (Fig. 2D). The kinase activity of LIMK1 and the phosphorylation of cofilin were not affected by the overexpression of wild-type LIMK1, which might be due to the high abundance of endogenous LIMK in the DRG.

Similar to the overexpression of T508V-LIMK1, intrathecal delivery of the other dominant-negative LIMK construct, T505V-LIMK2, increased the paw withdrawal latency of the ipsilateral paw, inhibited the kinase activity of LIMK2, and decreased the phosphorylation of cofilin in the ipsilateral DRG compared to the pEGFP control group (Fig. 2, E to H).

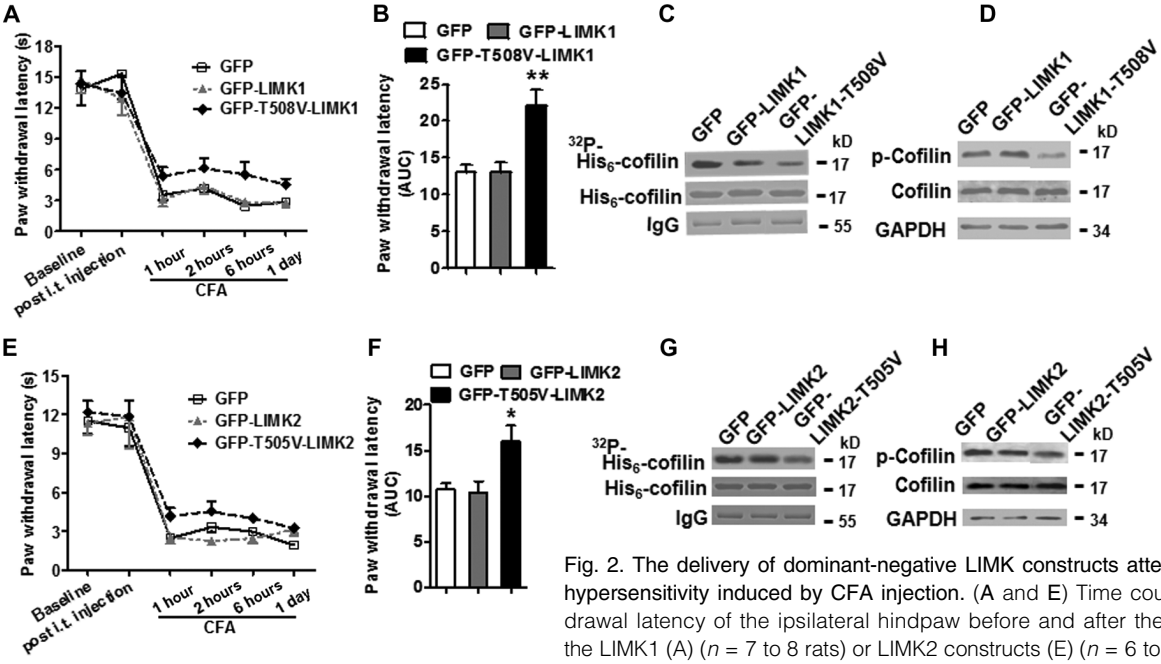

Fig. 2. The delivery of dominant-negative LIMK constructs attenuates pain hypersensitivity induced by CFA injection. (**A** and **E**) Time course of withdrawal latency of the ipsilateral hindpaw before and after the delivery of the LIMK1 (A) (n = 7 to 8 rats) or LIMK2 constructs (E) (n = 6 to 8 rats) after CFA injection. i.t., intrathecal. (**B** and **F**) Area under the curve (AUC) of the time course of the paw withdrawal latency in (A) and (E). (**C** and **G**) Changing Thr^{508} or Thr^{505} to valine decreased LIMK1 (C) or LIMK2 (G) activity in primary sensory neurons (n = 2 independent experiments). (**D** and **H**) Changing Thr^{508} or Thr^{505} to valine decreased the phosphorylation of cofilin (n = 2 independent experiments). The values in (A), (B), (E), and (F) represent the paw withdrawal latency (s) to radiant heat stimuli and refer to the means ± SEM. The data were analyzed by ANOVA followed by the Newman-Keuls multiple comparison test (*P < 0.05, **P < 0.01, compared with the group injected with GFP).

Knockdown of endogenous LIMK by short hairpin RNA reduced CFA-induced inflammatory heat hyperalgesia

We next examined paw withdrawal latency in rats that received intrathecal injections of short hairpin RNA (shRNA) plasmids directed against LIMK. Rats with knockdown of LIMK1 showed significantly increased withdrawal latency in the ipsilateral paw, but no change in basal nociceptive responses (Fig. 3A). The area under the curve of the time course indicated that the knockdown of LIMK1 significantly attenuated CFA-induced heat hyperalgesia (Fig. 3B). Western blot analysis indicated that the intrathecal delivery of shRNA-LIMK1 partially attenuated the expression of LIMK1, but not of LIMK2, after the CFA injection.

To avoid off-target effects of shRNA-LIMK1, we generated shRNA-resistant LIMK1 (Fig. 3D) and performed rescue experiments. In transfected mouse neuroblastoma N2a cells, the LIMK1 shRNA knocked down wild-type LIMK1 but not the shRNA-resistant LIMK1 (Fig. 3E). The ability of the LIMK1 shRNA to attenuate CFA-induced heat hyperalgesia was reduced by co-delivery of the shRNA-resistant LIMK1 construct (Fig. 3F). This construct did not affect basal nociceptive responses (Fig. 3F). The area under the curve of the time course indicated that shRNA-LIMK1 caused attenuation of CFA-induced heat hyperalgesia, which was rescued by shRNA-resistant LIMK1 (Fig. 3G). Together, these data suggest that the inhibition of heat hyperalgesia is due to the on-target effects of the shRNA vectors on the corresponding target mRNAs.

Similar to LIMK1 knockdown, expression of shRNA-LIMK2 decreased LIMK2 protein abundance in the DRG and increased the withdrawal latency of the ipsilateral paw during CFA-induced inflammatory pain when compared to the GFP control group (Fig. 4, A to C). Expression of shRNA-resistant LIMK2 rescued the increased withdrawal latency of the ipsilateral paw caused by the LIMK2 shRNA (Fig. 4, D to G).

Overall, our data suggest that shRNAs directed against LIMK reduced LIMK abundance in the DRG in vivo, which significantly attenuated behavioral nociception in the CFA-induced inflammatory pain model, indicating that LIMK activity is involved in heat hyperalgesia.

LIMK promotes CFA-induced heat hyperalgesia through the phosphorylation of cofilin

In contrast to other kinases that have multiple substrates, LIMKs have only one major substrate, the actin depolymerizing and severing protein cofilin (*20*, *21*). Our results showed that the phosphorylation of cofilin at Ser[3] increased significantly in the ipsilateral DRG after CFA treatment and that the intrathecal injection of dominant-negative forms of LIMK1 and LIMK2 reduced the phosphorylation of cofilin at Ser[3]. We hypothesized that LIMK modulates heat hyperalgesia through the phosphorylation of cofilin. To investigate this hypothesis, we used a synthetic peptide Tat-S3, which contains the unique Ser[3] phosphorylation site of cofilin in its C terminus

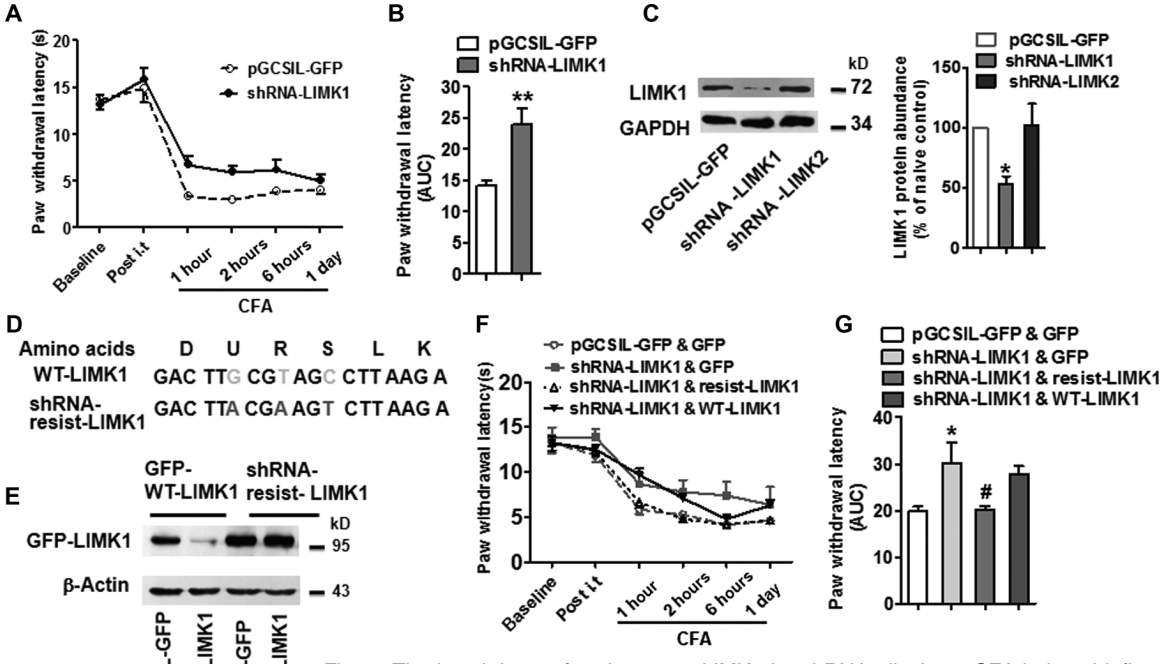

Fig. 3. The knockdown of endogenous LIMK1 by shRNA alleviates CFA-induced inflammatory heat hyperalgesia. (**A**) Effect of the knockdown of LIMK1 on CFA-induced inflammatory heat hyperalgesia (n = 9 to 13 rats). The values represent the paw withdrawal latency (s) to radiant heat stimuli and refer to the means ± SEM. (**B**) Area under the curve of the time course of the paw withdrawal latency in (A). $^{**}P < 0.01$, unpaired Student's t test compared with the pGCSIL-GFP group. (**C**) Knockdown of LIMK1 in DRG by the intrathecal injection of shRNA-LIMK1 1 hour after the CFA injection (n = 3 independent experiments). (**D**) The indicated amino acids were mutated to produce shRNA-resistant LIMK1. (**E**) shRNA-LIMK1 knocked down wild-type LIMK1 (WT-LIMK1), but not shRNA-resistant LIMK1, in mouse neuroblastoma N2a cells (n = 2 independent experiments). (**F**) Effect of shRNA-resistant LIMK1 on the effect of shRNA on CFA-induced inflammatory heat hyperalgesia (n = 7 to 13 rats). (**G**) Area under the curve of the time course of the paw withdrawal latency in (F). In (C) and (G), the graphs present the means ± SEM. The data were analyzed by ANOVA followed by the Newman-Keuls multiple comparison test ($^{*}P < 0.05$, compared with the corresponding control groups; $^{\#}P < 0.05$, compared with the shRNA-LIMK1 and WT-LIMK1 groups).

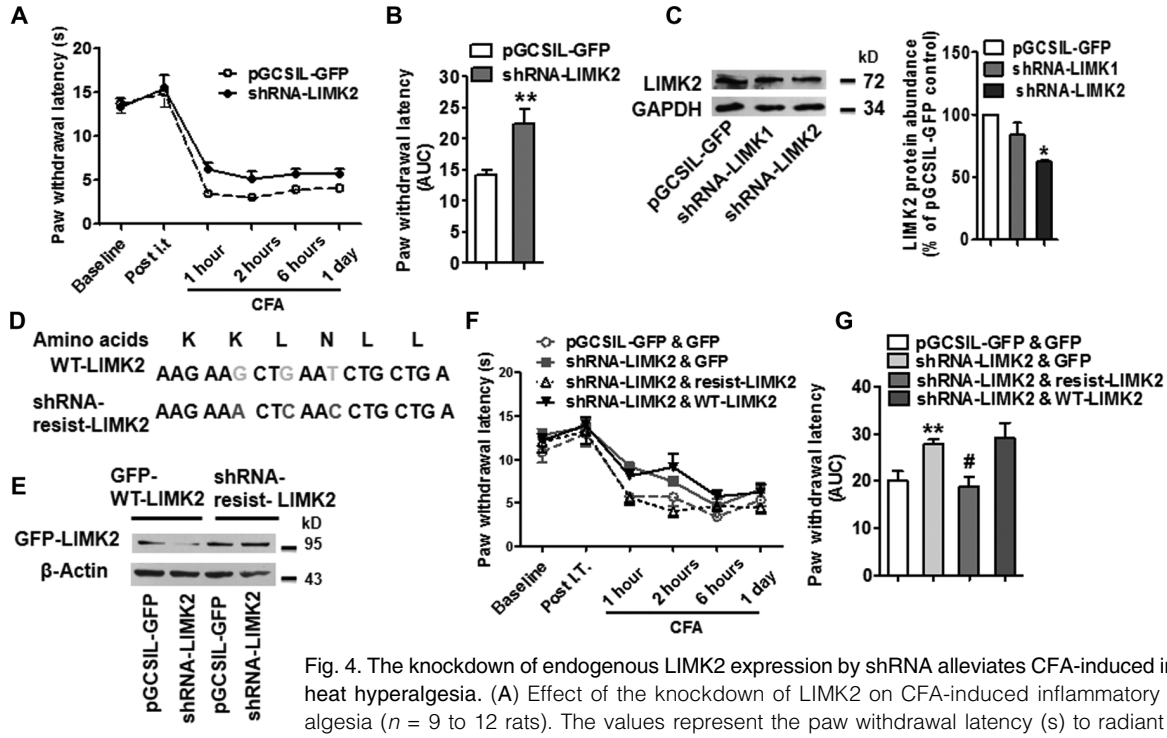

Fig. 4. The knockdown of endogenous LIMK2 expression by shRNA alleviates CFA-induced inflammatory heat hyperalgesia. (**A**) Effect of the knockdown of LIMK2 on CFA-induced inflammatory heat hyperalgesia (n = 9 to 12 rats). The values represent the paw withdrawal latency (s) to radiant heat stimuli and refer to the means ± SEM. (**B**) Area under the curve of the time course of the paw withdrawal latency in (A) (**P < 0.01, unpaired Student's t test compared with the pGCSIL-GFP group). (**C**) Knockdown of LIMK2 in the DRG by the intrathecal injection of shRNA-LIMK2 1 hour after the CFA injection (n = 3 independent experiments). (**D**) Indicated amino acids were mutated to produce shRNA-resistant LIMK2. (**E**) shRNA-LIMK2 knocked down WT-LIMK2, but not shRNA-resistant LIMK2, in mouse neuroblastoma N2a cells (n = 2 independent experiments). (**F**) shRNA-resistant LIMK2 rescued the effect of shRNA CFA-induced inflammatory heat hyperalgesia (n = 6 to 9 rats). (**G**) Area under the curve of the time course of the paw withdrawal latency in (F). In (C) and (G), the columns represent the means ± SEM. The data were analyzed by ANOVA followed by the Newman-Keuls multiple comparison test (*P < 0.05, **P < 0.01, compared with corresponding control groups; $^{\#}P$ < 0.05, compared with the group injected with shRNA-LIMK1 and WT-LIMK1).

and a cell-penetrating sequence in the N terminus to allow for neuronal internalization of the peptide. Consequently, this peptide can competitively inhibit the phosphorylation of cofilin at Ser^3 by LIMK. The Tat-S3A peptide, in which Ser^3 is mutated to Ala, was used as a control (Fig. 5A).

The Tat-S3 peptide did not affect basal nociceptive responses (Fig. 5B). Injection of the Tat-S3A peptide did not affect CFA-induced inflammatory heat hyperalgesia (Fig. 5C). In contrast, pretreatment with the Tat-S3 peptide attenuated CFA-induced inflammatory heat hyperalgesia in a dose-dependent manner, and the analgesic effect peaked at 1 hour at the 30-μg dose (Fig. 5, D to I).

The Tat-S3 peptide effectively inhibited the phosphorylation of cofilin at Ser^3 in the ipsilateral DRG in a dose-dependent manner without affecting the total protein abundance of cofilin (Fig. 5, J and K). Thus, we conclude that intrathecal pretreatment with the S3 peptide, which interferes with the phosphorylation of cofilin by LIMK, markedly attenuates CFA-induced heat hyperalgesia.

Actin dynamics regulated by LIMK are involved in CFA-induced inflammatory heat hyperalgesia

The cytoskeleton is a dynamic, plastic system involved in compartmentalizing and modulating cell signaling (*5*). To examine the role of actin microfilaments in CFA-induced heat hyperalgesia, we injected the actin microfilament-disrupting agent latrunculin A (Lat A) intradermally and intrathecally before the CFA injection. Lat A significantly attenuated CFA-induced heat hyperalgesia (Fig. 6, A to D). These results show that actin microfilaments play a similar role both in CFA-induced hyperalgesia and in hyperalgesia induced by epinephrine (*5*). It might act as a scaffold for components of signaling pathways activated by CFA, such as receptors and downstream kinases, such as PKA, PKC, and ERK1/2, and their effectors.

Actin microfilament dynamics and reorganization are spatiotemporally regulated by numerous actin-binding proteins. The ADF/cofilin family of proteins can sever and depolymerize F-actin and increase the cellular concentration of monomeric globular actin (G-actin) (*48*). Actin polymerization assays indicated that CFA injection significantly stimulated actin polymerization to F-actin in the ipsilateral DRG (Fig. 6E). The polymerized F-actin could link components of signaling pathways activated by CFA. Conversely, the knockdown of LIMK decreased the amount of F-actin in the ipsilateral DRG compared to the GFP control group (Fig. 6F). These results suggest that the polymerization of actin is involved in transducing CFA-induced inflammatory pain and that the knockdown of LIMK causes actin reorganization during pain hypersensitization.

TRPV1 is a downstream effector of the LIMK-cofilin signaling pathway–dependent actin dynamics in inflammatory hyperalgesia

The TRPV1 channel is an ion channel that mediates inflammatory thermal nociception and is present on sensory neurons. Knockout mice lacking

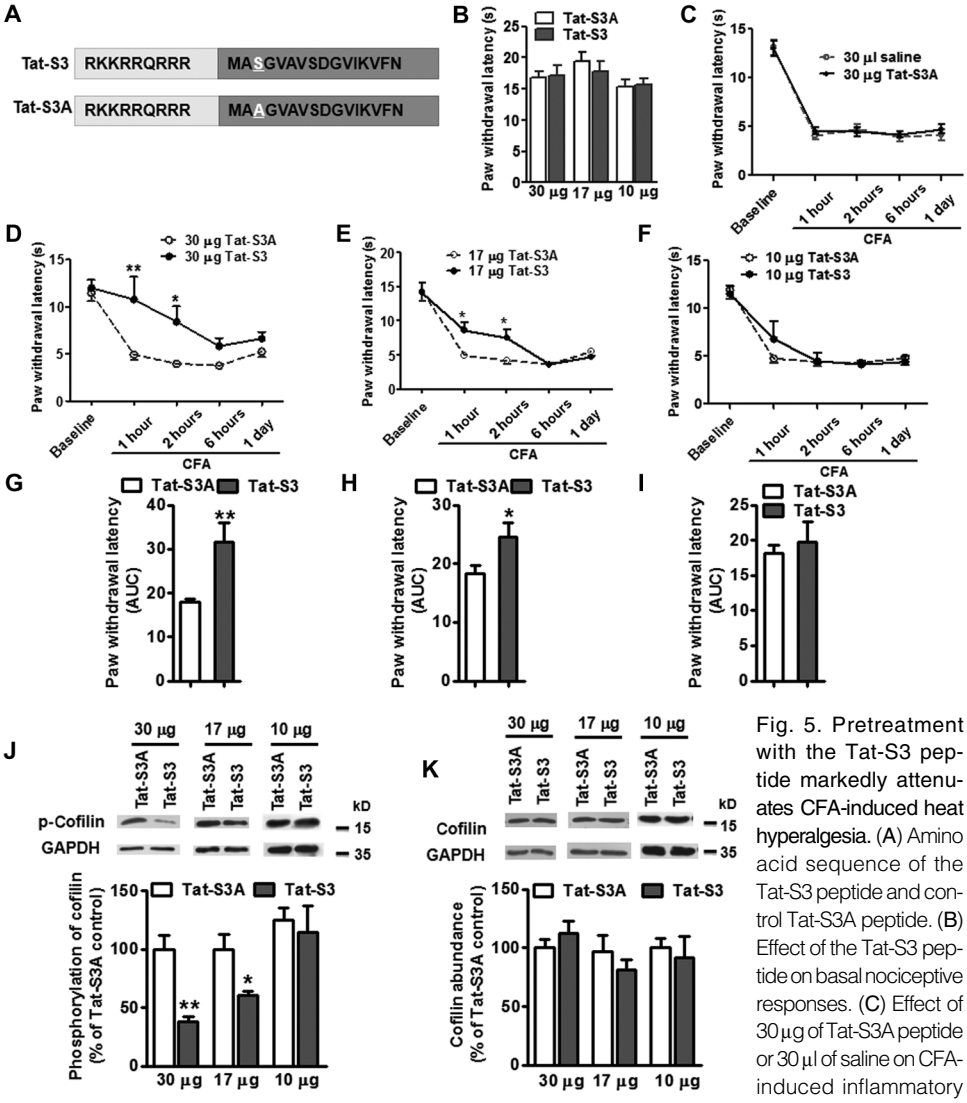

Fig. 5. Pretreatment with the Tat-S3 peptide markedly attenuates CFA-induced heat hyperalgesia. (A) Amino acid sequence of the Tat-S3 peptide and control Tat-S3A peptide. (B) Effect of the Tat-S3 peptide on basal nociceptive responses. (C) Effect of 30 µg of Tat-S3A peptide or 30 µl of saline on CFA-induced inflammatory heat hyperalgesia. (D to F) Time course of withdrawal latency of the ipsilateral hindpaw before and after the intrathecal injection of 30 µg ($n = 7$ rats, $P = 0.6684$), 17 µg ($n = 11$ rats, $P = 0.0350$), or 10 µg ($n = 8$ to 9 rats, $P = 0.0001$) of the Tat-S3 peptide or the Tat-S3A peptide after CFA injection. The values represent the paw withdrawal latency (s) to radiant heat stimuli and refer to the means ± SEM (*$P < 0.05$, **$P < 0.01$, two-way ANOVA, followed by Bonferroni posttests, compared with the Tat-S3A peptide group at corresponding time points). (G to I) Area under curve of the time course of the paw withdrawal latency (*$P < 0.05$, **$P < 0.01$, unpaired Student's *t* test, compared with the Tat-S3A peptide group). (J and K) Pretreatment with 30 µg of the Tat-S3 peptide, but not the Tat-S3A peptide, reduced the phosphorylation of cofilin in vivo (J) without affecting cofilin abundance (K). The columns represent the means ± SEM from three separate experiments (*$P < 0.05$, **$P < 0.01$, unpaired Student's *t* test, compared with Tat-S3A peptide group).

TRPV1 do not develop heat hyperalgesia after inflammation (*51*, *52*). TRPV1 abundance is increased in the DRG, the sciatic nerve, and the hindpaw skin after CFA-induced inflammatory pain (*53*, *54*). After inflammation, various extracellular mediators, including bradykinin, prostaglandin E_2, and NGF, are released, which lowers the heat activation threshold of TRPV1 by activating kinases such as PKA, PKCε, and ERK1/2, which phosphorylate TRPV1 (*41–45*, *55*). A kinase anchoring protein 79 (AKAP79) has binding sites for both PKA and PKC and is distributed with TRPV1 in small nociceptive sensory neurons (*56*, *57*). AKAP79 binds to TRPV1 and is essential for PKA- and PKC-dependent sensitization of TRPV1 (*56*, *58–60*). In addition, AKAP79 supports the interactions between PKA, PKCε, and F-actin (*37–40*). Therefore, we hypothesized that LIMK-cofilin-actin signaling may modulate the function of the TRPV1 channel.

Fura-2 AM Ca^{2+} imaging of acutely dissociated DRG neurons from rats that received CFA injections in the left hindpaw showed that the shRNA-induced knockdown of LIMK before CFA injections reduced the rapid, robust increase in intracellular Ca^{2+} in neurons stimulated with capsaicin, which activates TRPV1 (Fig. 7, A and B). Furthermore, intrathecal pretreatment of rats with the Tat-S3 peptide also significantly lowered the TRPV1 response to capsaicin compared with the Tat-S3A peptide (Fig. 7, C and D). Thus, TRPV1 channel function was impaired by the knockdown of LIMK and inhibition of cofilin phosphorylation, both of which resulted in F-actin depolymerization. The knockdown of LIMK alone slowed the intracellular Ca^{2+} increase, and the Tat-S3 peptide not only slowed the intracellular Ca^{2+} increase but also reduced the amplitude of intracellular Ca^{2+}, suggesting that the Tat-S3 peptide might be more efficacious than LIMK knockdown. The behavioral responses also support this hypothesis (Figs. 2B, 3B, and 5D).

To detect whether the function of TRPV1 was modulated through phosphorylation, which is related to actin dynamics, we detected the serine phosphorylation of TRPV1 in the ipsilateral DRG after CFA treatment alone or combined with the Tat-S3 or the Tat-S3A peptide. The serine phosphorylation of TRPV1 was significantly increased after CFA injection (Fig. 7E), an increase that was reduced by the Tat-S3 peptide (Fig. 7F). These results indicate that TRPV1 channel function is enhanced through its phosphorylation and that the F-actin regulated by LIMK may act as a scaffold.

DISCUSSION

The present study provides evidence that LIMK-dependent actin polymerization in the primary sensory neurons is involved in the development of inflammatory hyperalgesia in rats and that TRPV1 may function as one of the downstream effectors in this process.

NGF plays a major role in the production of inflammatory hyperalgesia (*34*, *54*, *61*). Several types of cells release NGF. During CFA-induced inflammatory pain, NGF synthesis and release increase in peripheral tissue. NGF binds to tyrosine kinase receptor A (TrkA) in nociceptive afferent nerve fibers and increases the activation of the primary nociceptive receptor

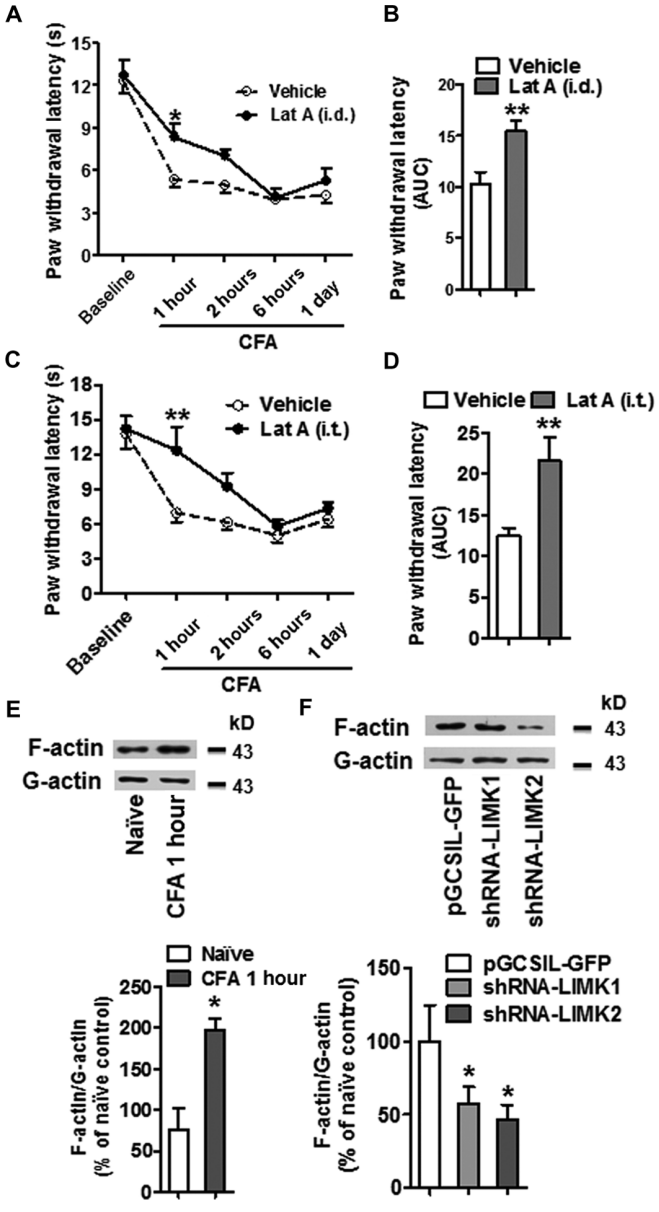

Fig. 6. The role of actin filaments in CFA-induced heat hyperalgesia. (A to D) Time course of the withdrawal latency of the ipsilateral hindpaws before and after the intradermal (i.d.) (A) (500 ng, $n = 8$ rats) or intrathecal (C) (100 ng, $n =$ 10 to 11 rats) injection of Lat A after CFA injection (A and C), and the area under the curve of the time course of the paw withdrawal latency (B and D). The values represent the paw withdrawal latency (s) to radiant heat stimuli and refer to the means ± SEM (**$P < 0.01$, two-way ANOVA, followed by Bonferroni post-tests, compared with the vehicle group at corresponding time points, and unpaired Student's t test, compared with the vehicle group). (E) Representative Western blot for G- and F-actin in the DRG before and after CFA injection, and quantification of the relative F-actin/G-actin ratio (*$P < 0.05$, unpaired Student's t test, compared with naïve group) ($n = 3$ independent experiments). (F) Effect of the knockdown of LIMK on the relative F-actin/G-actin ratio after CFA injection. The relative densitometry of the intensity of G- and F-actin bands and the ratio of F-actin/G-actin were measured for each condition (*$P < 0.05$, ANOVA followed by the Newman-Keuls multiple comparison test, compared with pGCSIL-GFP groups) ($n = 3$ independent experiments).

TRPV1 (*34*, *62*). Trk receptor signaling activates several small G proteins (heterotrimeric guanine nucleotide–binding proteins), including those in the Cdc42-Rac-Rho family (*63*). Various Rho GTPase effectors activate LIMK1 and LIMK2 by phosphorylating conserved threonine residues in the LIMK activation loop (*12–19*, *64*). Together, these findings suggest that in CFA-induced inflammatory pain, NGF can activate Rho GTPases and their effectors and subsequently stimulate the activity of LIMK1 and LIMK2.

In addition, MAPKAPK-2 [MK2, a kinase downstream of p38 MAPK (mitogen-activated protein kinase)] activates LIMK1 by phosphorylating Ser^{323} (*65*). The phosphorylation of Ser^{323} might induce a conformational change in LIMK1, releasing the autoinhibitory effect of the N-terminal region and increasing the kinase activity of LIMK1. Peripheral inflammation induces the activation of ERK and p38 in the DRG (*54*, *66*), and the Ras/B-Raf/MEK (MAPK kinase)/ERK signaling pathway increases the activity of the Rho effector ROCK (*67*), which in turn stimulates LIMK activity. To elucidate the downstream molecular mechanisms of the role of LIMK in the modulation of heat hyperalgesia, we performed intrathecal injections with a Tat-S3 peptide designed according to a previous study (*25*). Many studies have confirmed that the S3 peptide efficiently inhibits the phosphorylation of cofilin at Ser^3 in vitro and in vivo. In our study, to increase the ability of the peptide to penetrate membranes, we changed the penetrating sequence to the HIV Tat protein sequence. Pretreatment with the Tat-S3 peptide efficiently reduced the phosphorylation of cofilin in the DRG and markedly alleviated CFA-induced heat hyperalgesia. These results indicate that cofilin might be the substrate of LIMK involved in the modulation of hyperalgesia.

In normal male rats, intact actin filaments, microtubules, and intermediate filaments are all necessary for epinephrine-induced inflammatory hyperalgesia (*5*). In our study, we also found that intact actin filaments were necessary for the development of CFA-induced inflammatory pain. Furthermore, we found that CFA stimulation induced actin polymerization and that both the knockdown of LIMK and the inhibition of cofilin phosphorylation decreased the relative amount of F-actin, suggesting that the activity of LIMK is essential for actin polymerization during the development of CFA-induced inflammatory pain.

Many protein kinases that play important roles in pain transmission, including PKA, PKCε, and ERK1/2 of the MAPK family, interact with the cytoskeleton and depend on the intact cytoskeleton for signal transmission (*68–72*). PKCε binds to F-actin in a phorbol ester–dependent manner, and purified F-actin can directly stimulate PKCε kinase activity in vitro. In PMA (phorbol 12-myristate 13-acetate)–treated, PKCε-overexpressing NIH 3T3 cells, activated PKCε and F-actin redistribute to the cell margins, typically in areas of cell-cell contact (*36*). The AKAP family of scaffolding proteins is present in sensory neurons and can potentially support interactions between β-adrenergic receptors, PKA, PKCε, and F-actin (*35*, *37–40*). The β-adrenergic receptor mediates the activation of ERK1/2 through several signaling scaffolds that associate with the cytoskeleton. The PKA regulatory subunit localizes to F-actin microspikes in hippocampal growth cones in an AKAP-independent manner (*73*). Together, these data suggest that F-actin can act as a scaffold that supports interactions among the receptors involved in pain signaling, downstream kinases, and their effectors.

TRPV1 plays a central role in the development of thermal hyperalgesia in inflammatory pain. Inflammatory mediators such as prostaglandin E_2 or bradykinin cause hyperalgesia by activating cellular kinases that phosphorylate TRPV1, a process that relies on AKAP79/150 to target the kinases to TRPV1 (*56*, *58*, *59*). A peptide mimicking the TRPV1 binding site for AKAP79 blocks TRPV1 sensitization in vitro and inflammatory pain in vivo (*60*). The modulation of TRPV1 sensitivity by PKA and PKC and by the phosphatase calcineurin depends on the formation of a signaling

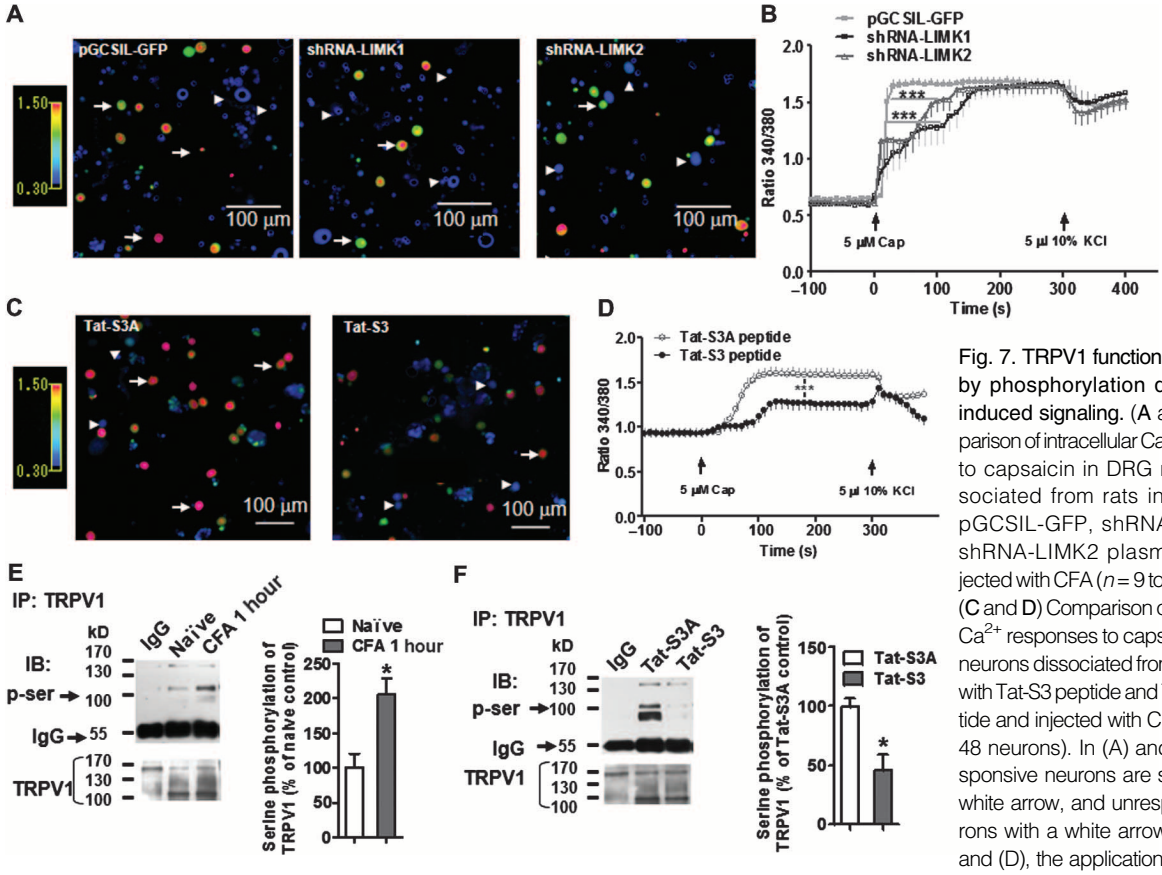

Fig. 7. TRPV1 function is enhanced by phosphorylation during CFA-induced signaling. (**A** and **B**) Comparison of intracellular Ca^{2+} responses to capsaicin in DRG neurons dissociated from rats injected with pGCSIL-GFP, shRNA-LIMK1, or shRNA-LIMK2 plasmids and injected with CFA ($n = 9$ to 15 neurons). (**C** and **D**) Comparison of intracellular Ca^{2+} responses to capsaicin in DRG neurons dissociated from rats treated with Tat-S3 peptide and Tat-S3A peptide and injected with CFA ($n = 44$ to 48 neurons). In (A) and (C), the responsive neurons are shown with a white arrow, and unresponsive neurons with a white arrowhead. In (B) and (D), the application of capsaicin and KCl is shown with an arrow (***$P < 0.001$, two-way ANOVA, followed by Bonferroni posttests, compared with corresponding control groups). (**E** and **F**) Serine phosphorylation of TRPV1 in anti-TRPV1 immunoprecipitates from DRG extract after CFA injection (E) and the effect of the Tat-S3 peptide (F). The graphs present the means ± SEM from three separate experiments (*$P < 0.05$, unpaired Student's *t* test, compared with corresponding control groups).

complex of these enzymes, the scaffolding protein AKAP79/150, and TRPV1 (*56*). Here, we found that the phosphorylation of serines in TRPV1 was increased after CFA injection, an effect that was reduced by inhibition of cofilin phosphorylation. These results suggest that TRPV1 may be an effector of the downstream kinases in CFA-induced inflammatory hyperalgesia.

In summary, this study demonstrates a pivotal role of LIMK, a key regulator of actin dynamics in the development of inflammatory heat hyperalgesia. Peripheral inflammation results in the activation of LIMK in the DRG, and phosphorylation and inactivation of cofilin by LIMK promote actin polymerization. The polymerized F-actin may act as a scaffold for inflammatory signaling and downstream kinases and their effectors, such as TRPV1, which could facilitate the phosphorylation of TRPV1 by these kinases, leading to the enhanced function of TRPV1 channels.

MATERIALS AND METHODS

Animals

Male Sprague-Dawley rats weighing 200 to 220 g were supplied by the Animal Center of Peking University Health Science Center. The animals were housed in climate-controlled rooms on a 12-hour light-dark cycle with free access to food and water. Experimental procedures were approved by the Animal Care and Use Committee of Peking University, and all efforts were made to minimize the discomfort of the animals. First, 25% CFA (100 μl, F5881, Sigma-Aldrich) diluted in incomplete Freund's adjuvant (iFA, F5506, Sigma-Aldrich) was injected into the plantar surface of the left hindpaw while the animals were under isoflurane anesthesia. The rats were then sacrificed 0.5 hour, 1 hour, 2 hours, 6 hours, or 1 day after the injection under 10% chloral hydrate anesthesia [0.3 g/kg, intraperitoneally (ip)], and tissues were dissected.

For intrathecal drug delivery, the cannulae implantation was performed following the method of Størkson *et al.* (*74*). Briefly, rats were anesthetized with 10% chloral hydrate (0.3 g/kg, ip). The back skin of the rats was incised, and the spinal column was exposed. The needle was inserted into the intraspinal space between L4 and L5. The correct intrathecal location was confirmed by a tail flick or a paw retraction. PE-10 polyethylene catheters 3.5 to 4.0 cm in length were implanted using a catheter-through-needle technique to reach the lumbar enlargement of the spinal cord. The outer end of the catheter was plugged and fixed to the skin upon closure of the wound. The rats were individually housed after surgery and allowed to recover for 4 to 6 days before being tested. Any animals showing motor impairment from the intrathecal cannula placement were excluded from the study. For the experiments involving genes and peptide, 100% CFA was diluted to 25% in iFA to avoid excessive inflammation and spontaneous pain behavior. Nociceptive responses after intrathecal injection or delivery of the genes were measured in a blinded fashion.

Assessment of hypersensitivity

Thermal hyperalgesia was assessed in unrestrained rats using a procedure adapted from a previously published report (*46*). Briefly, the animals were allowed to become accustomed to the environment for 20 min before testing. Their paw withdrawal latency in response to radiant heat was recorded. A cutoff time of 30 s was enforced to prevent tissue damage. The paw withdrawal latency was recorded and averaged over four trials at 5-min intervals.

Plasmids and constructs

LIMK1 and LIMK2 were amplified from the rat complementary DNA (cDNA) library using primers with the sequences 5′-AGCAGATCTCGATGAGGTTCACGCTACTT-3′ (LIMK1 5′ end); 5′-AGCCTCGAGCATGGCGGCGCTGGCGGGT-3′ (LIMK2 5′ end); 5′-AGCAAGCTTTTTCAGTCAGGGACCTCGGG-3′ (LIMK1 3′ end); and 5′-AGCGGATCCACCTAGGGTGGCTAGTCCCG-3′ (LIMK2 3′end). The amplified sequences were subcloned into the pEGFP-C2 vector (Clontech). Dominant-negative LIMK1 (T508V-LIMK1) (*11*, *17*) and dominant-negative LIMK2 (T505V-LIMK2) (*16*) were prepared by mutating Thr to Val in the pEGFP-C2 LIMK1 or pEGFP-C2 LIMK2 plasmids. Mutagenesis was performed with the QuikChange Site-Directed Mutagenesis Kit (Stratagene). All of the constructs were verified by sequencing performed by Shanghai Sangon Biological Engineering Technology and Services Co. Ltd.

The shRNA plasmids were generated by Shanghai Genechem Co. Ltd. Oligonucleotides targeting LIMK1 and LIMK2 were ligated to the vector pGCSIL-GFP. The shRNA sequence for rat LIMK1 is 5′-GACTTGCGTAGCCTTAAGA-3′ and that for LIMK2 is 5′-GGACAAGAAGCTGAATCTG-3′. For the rescue experiments, the third base of each codon in the target sequence was mutated without changing the identity of the amino acids.

Western blotting

Rats were deeply anesthetized with 10% chloral hydrate (0.3 g/kg, ip), and the L4-L6 DRG and the dorsal horn of the lumbar enlargement of the spinal cord were subsequently removed and immediately homogenized in ice-cold lysis buffer [50 mM tris at pH 7.4, 150 mM NaCl, 1.5 mM $MgCl_2$, 10% glycerol, 1% Triton X-100, 5 mM EGTA, 1 mM phenylmethylsulfonyl fluoride, 1 mM Na_3VO_4, 10 mM NaF, and a proteinase inhibitor cocktail purchased from AMRESCO (0.5 mM AEBSF, 0.3 μM aprotinin, 10 μM bestatin, 10 μM E-64, 10 μM leupeptin)]. The homogenates were centrifuged at 12,000*g* for 5 min at 4°C, and the supernatant was analyzed. The protein concentration was measured using a BCA assay kit (Pierce Biotechnology). Next, 50 μg of each sample was boiled for 5 min with SDS–polyacrylamide gel electrophoresis (SDS-PAGE) sample buffer and subjected to SDS-PAGE using 12% running gels and transferred onto nitrocellulose membranes. The membranes were blocked with 5% nonfat milk in TBST (50 mM tris-HCl at pH 7.5, 150 mM NaCl, and 0.05% Tween 20) for 1 hour at room temperature and then incubated overnight at 4°C with the primary antibody. The blots were then washed three times in TBST for 10 min each. Next, the membranes were incubated with horseradish peroxidase–conjugated secondary antibody (1:2000 dilution; goat anti-rabbit, rabbit anti-goat, or goat anti-mouse; Bio-Rad Laboratories) for 1 hour at room temperature. Finally, the blots were developed with the lightening chemiluminescence kit (sc-2048; Santa Cruz Biotechnology).

The following commercial antibodies were used as primary antibodies: LIMK1 (1:100, sc-5576; Santa Cruz Biotechnology), LIMK2 (1:100, sc-8388; Santa Cruz Biotechnology), cofilin (1:100, sc-33779; Santa Cruz Biotechnology), p-cofilin (Ser^3) (1:2000, sc-12912-R/sc-21867-R; Santa Cruz Biotechnology), GAPDH (glyceraldehyde-3-phosphate dehydrogenase) (1:2000, CW0100; CoWin Biotech Co. Ltd.), SSH1L (C-terminal region) (1:800, SP1711; ECM Biosciences), and SSH1L (Ser^{978}) (1:800, SP3901; ECM Biosciences).

In vitro kinase assay

LIMK1 and LIMK2 kinase activities were measured using an immune complex kinase assay and His_6-cofilin as the substrate, as previously described. Briefly, tissue lysates were immunoprecipitated with anti-LIMK1 or anti-LIMK2 antibodies (1:50) at 4°C for 3 hours. Protein A–Sepharose CL-4B resin (Amersham Biosciences) was added to the samples and incubated for an additional 12 hours, after which the samples were washed four times with TBS (tris-buffered saline)/0.1% Triton X-100 and two times with the assay buffer (20 mM tris-HCl at pH 7.6, 20 mM $MgCl_2$). The final pellet was resuspended in a reaction buffer [20 mM tris-HCl at pH 7.6, 20 mM $MgCl_2$, 0.1 mM dithiothreitol, [γ-^{32}P]ATP (10 μCi/50 μl), His_6-cofilin] to yield a total volume of 40 μl. The mixture was then incubated at 30°C for 30 min, and the reaction was terminated by the addition of SDS-PAGE sample buffer. The samples were boiled for 5 min and then subjected to SDS-PAGE. The gels were stained with Coomassie blue, dried, and exposed to x-ray film for autoradiography.

Delivery of constructs into the DRG

After 4 to 6 days of surgical recovery from the intrathecal catheter placement, the rats were randomly assigned to different experimental groups: pEGFP-LIMK1, pEGFP-T508V-LIMK1, and pEGFP, or shRNA-LIMK1, shRNA-LIMK2, and pGCSIL-GFP. The basal paw withdrawal latency was measured before the rats were subjected to intrathecal injection of the plasmids. Complexes of DNA and Lipofectamine 2000 (Invitrogen), prepared as described below, were slowly injected over 5 min. After the injection, the needle remained in situ for 2 min before withdrawal. The basal paw withdrawal latency was then measured 4 days after gene delivery, and 25% CFA was subsequently injected into the plantar surface of the left hindpaw. The nociceptive responses were then measured 1 hour, 2 hours, 6 hours, and 1 day after CFA administration. DNA–Lipofectamine 2000 complexes were prepared as follows: DNA (10 μg, 1 μg/μl) was diluted in normal saline (10 μl) and gently mixed. Next, Lipofectamine 2000 (20 μl) was added to normal saline (10 μl) and mixed gently. After 5 min of incubation at room temperature, the diluted DNA was combined with the diluted Lipofectamine 2000, mixed, and incubated for 20 min at room temperature to allow DNA–Lipofectamine 2000 complexes to form. The mixture was then intrathecally injected. The ratio of DNA (in μg) to Lipofectamine 2000 (in μl) was 1:2 (for cotransfection: the ratio was 1:1). The total volume injected was 50 μl.

Peptides and treatments

The Tat-S3 peptide (RKKRRQRRR MASGVAVSDGVIKVFN) and the control Tat-S3A peptide (RKKRRQRRR MAAGVAVSDGVIKVFN) were synthesized and purified by the Chinese Peptide Company. The peptides were dissolved in sterile double-distilled water (ddH_2O) to a final concentration of 1 μg/μl.

After 4 to 6 days of surgical recovery from the placement of the intrathecal catheter, the rats were randomly placed into the Tat-S3 or Tat-S3A peptide group. The basal paw withdrawal latency was measured, and the rats were subjected to an intrathecal injection of the peptides at different dosages: 10 μg, 17 μg, 30 μg; 1 μg/μl. After injection, the needle remained in situ for 2 min before withdrawal. The basal paw withdrawal latency was measured 0.5 hour after the peptide injection, and then 25% CFA was injected into the plantar surface of the left hindpaw. Nociceptive responses were measured again 1 hour, 2 hours, 6 hours, and 1 day after CFA administration.

F-actin/G-actin in vivo assay

The ratio of F-actin to G-actin in the DRG after treatment with CFA, peptide, or shRNA plasmids was analyzed using an F-actin/G-actin in vivo assay kit (BK037, Cytoskeleton Inc.). Briefly, the rats were deeply anesthetized with 10% chloral hydrate (0.3 g/kg, ip). Next, the L4-L6 DRG was removed and immediately homogenized with a motorized homogenizer

in F-actin stabilization buffer. The tissue lysates were centrifuged at 100,000*g*, 37°C, for 1 hour; the resulting pellet contained the F-actin, and the supernatant contained the G-actin. The supernatant was removed and immediately placed on ice, and 100 μl of F-actin depolymerization buffer was added to each pellet. The samples were then incubated on ice for 1 hour. Equal volumes of G-actin and F-actin samples were mixed with SDS-PAGE sample buffer, electrophoresed in separate lanes on a 12% SDS-PAGE gel, and subjected to immunoblot analysis.

Isolation of DRG neurons and Ca^{2+} imaging

The isolation of DRG neurons and Fura-2 AM–based Ca^{2+} imaging experiments were performed as described previously (*75*). After 4 to 6 days of surgical recovery from the placement of the intrathecal catheter, the plasmids (pGCSIL-GFP, shRNA-LIMK1, and shRNA-LIMK2) or the peptides (Tat-S3 peptide and Tat-S3A peptide, 30 μg, 1 μg/μl) were delivered into the DRG. One hour after the CFA injection, the rats were terminally anesthetized with 10% chloral hydrate (0.3 g/kg, ip), and then the left L4-L5 DRG was removed and digested with collagenase type IA (1.5 mg/ml; Sigma-Aldrich) for 40 to 50 min and then with 0.125% trypsin (Sigma-Aldrich) for 8 to 10 min at 37°C. The enzymatic treatment was terminated by the addition of DMEM (Dulbecco's modified Eagle's medium) followed by gentle trituration of the ganglia with a flame-polished Pasteur pipette and centrifugation at 500 rpm for 5 min. The cell pellet was then resuspended in DMEM. The dissociated cells were plated on poly-D-lysine–coated (100 μg/ml; Sigma-Aldrich) glass coverslips inside 35-μm culture dishes with a 10-mm bottom well and kept for 1.5 hours at 37°C in an incubator with 5% CO_2 and 95% air.

The DRG cells were washed with extracellular solution (ES) (7.605 g of NaCl, 0.3725 g of KCl, 0.272 g of KH_2PO_4, 0.094 g of $MgCl_2$, 0.2775 g of $CaCl_2$, 1.8 g of glucose, and 2.38 g of Hepes, dissolved in 1000 ml of ddH_2O, pH 7.4 to 7.6, 300 mOsm) twice and then incubated in Fura-2 AM (5 μM; Invitrogen) in ES at room temperature for 1 hour. The cells were then washed with ES and left in ES at room temperature in the dark for 1-hour recovery. For calcium imaging, an inverted fluorescence microscope equipped with a 340- and 380-nm excitation filter (Olympus) and a computer with the MetaFluor software were used. Fluorescent images and the F340/F380 ratio were acquired every 10 s. TRPV1 activation was evoked by the addition of 5 μM capsaicin.

Immunoprecipitation

For immunoprecipitation, protein extracts containing 400 to 500 μg of protein from the rats' DRG were incubated overnight at 4°C with a goat anti-TRPV1 antibody (1:100, sc-12498; Santa Cruz Biotechnology) or normal goat immunoglobulin G (1:200, sc-2028; Santa Cruz Biotechnology) with protein A–Sepharose CL-4B resin (GE Healthcare) in a volume of 500 μl. The samples were then washed six times with TBS/0.1% Triton X-100 to solubilize bound proteins. The proteins in the TRPV1 precipitates were resolved by 10% SDS-PAGE, and the serine phosphorylation was detected by Western blot analysis using a mouse anti-phosphoserine antibody (1:200, sc-81515; Santa Cruz Biotechnology).

Statistical analysis

All of the data are represented as the means ± SEM. Statistical analyses were performed with the Prism 5.0 software. Differences between groups were compared using either Student's *t* test, a one-way ANOVA followed by Newman-Keuls post hoc tests, or a two-way ANOVA followed by Bonferroni post hoc tests. Statistical significance was set at $P < 0.05$. For the Western blot analysis, films were scanned using the Quantity One software, and the densities of specific bands were measured and normalized with an internal loading control band.

REFERENCES AND NOTES

1. B. M. Riederer, S. R. Goodman, Association of brain spectrin isoforms with microtubules. *FEBS Lett.* **277**, 49–52 (1990).
2. K. L. Lankford, W. L. Klein, Ultrastructure of individual neurons isolated from avian retina: Occurrence of microtubule loops in dendrites. *Brain Res. Dev. Brain Res.* **51**, 217–224 (1990).
3. T. B. Shea, M. L. Beermann, Respective roles of neurofilaments, microtubules, MAP1B, and tau in neurite outgrowth and stabilization. *Mol. Biol. Cell* **5**, 863–875 (1994).
4. L. J. Boyne, I. Fischer, T. B. Shea, Role of vimentin in early stages of neuritogenesis in cultured hippocampal neurons. *Int. J. Dev. Neurosci.* **14**, 739–748 (1996).
5. O. A. Dina, G. C. McCarter, C. de Coupade, J. D. Levine, Role of the sensory neuron cytoskeleton in second messenger signaling for inflammatory pain. *Neuron* **39**, 613–624 (2003).
6. G. Bhave, R. W. Gereau IV, Growing pains: The cytoskeleton as a critical regulator of pain plasticity. *Neuron* **39**, 577–579 (2003).
7. L. A. Cingolani, Y. Goda, Actin in action: The interplay between the actin cytoskeleton and synaptic efficacy. *Nat. Rev. Neurosci.* **9**, 344–356 (2008).
8. K. Mizuno, I. Okano, K. Ohashi, K. Nunoue, K. Kuma, T. Miyata, T. Nakamura, Identification of a human cDNA encoding a novel protein kinase with two repeats of the LIM/double zinc finger motif. *Oncogene* **9**, 1605–1612 (1994).
9. K. Ohashi, J. Toshima, K. Tajinda, T. Nakamura, K. Mizuno, Molecular cloning of a chicken lung cDNA encoding a novel protein kinase with N-terminal two LIM/double zinc finger motifs. *J. Biochem.* **116**, 636–642 (1994).
10. I. Okano, J. Hiraoka, H. Otera, K. Nunoue, K. Ohashi, S. Iwashita, M. Hirai, K. Mizuno, Identification and characterization of a novel family of serine/threonine kinases containing two N-terminal LIM motifs. *J. Biol. Chem.* **270**, 31321–31330 (1995).
11. D. C. Edwards, L. C. Sanders, G. M. Bokoch, G. N. Gill, Activation of LIM-kinase by Pak1 couples Rac/Cdc42 GTPase signalling to actin cytoskeletal dynamics. *Nat. Cell Biol.* **1**, 253–259 (1999).
12. U. K. Misra, R. Deedwania, S. V. Pizzo, Binding of activated α_2-macroglobulin to its cell surface receptor GRP78 in 1-LN prostate cancer cells regulates PAK-2-dependent activation of LIMK. *J. Biol. Chem.* **280**, 26278–26286 (2005).
13. H. Wu, Y. Zheng, Z. X. Wang, Evaluation of the catalytic mechanism of the p21-activated protein kinase PAK2. *Biochemistry* **42**, 1129–1139 (2003).
14. C. Dan, A. Kelly, O. Bernard, A. Minden, Cytoskeletal changes regulated by the PAK4 serine/threonine kinase are mediated by LIM kinase 1 and cofilin. *J. Biol. Chem.* **276**, 32115–32121 (2001).
15. T. Sumi, K. Matsumoto, A. Shibuya, T. Nakamura, Activation of LIM kinases by myotonic dystrophy kinase-related Cdc42-binding kinase α. *J. Biol. Chem.* **276**, 23092–23096 (2001).
16. T. Sumi, K. Matsumoto, T. Nakamura, Specific activation of LIM kinase 2 via phosphorylation of threonine 505 by ROCK, a Rho-dependent protein kinase. *J. Biol. Chem.* **276**, 670–676 (2001).
17. K. Ohashi, K. Nagata, M. Maekawa, T. Ishizaki, S. Narumiya, K. Mizuno, Rho-associated kinase ROCK activates LIM-kinase 1 by phosphorylation at threonine 508 within the activation loop. *J. Biol. Chem.* **275**, 3577–3582 (2000).
18. M. Maekawa, T. Ishizaki, S. Boku, N. Watanabe, A. Fujita, A. Iwamatsu, T. Obinata, K. Ohashi, K. Mizuno, S. Narumiya, Signaling from Rho to the actin cytoskeleton through protein kinases ROCK and LIM-kinase. *Science* **285**, 895–898 (1999).
19. T. Amano, K. Tanabe, T. Eto, S. Narumiya, K. Mizuno, LIM-kinase 2 induces formation of stress fibres, focal adhesions and membrane blebs, dependent on its activation by Rho-associated kinase-catalysed phosphorylation at threonine-505. *Biochem. J.* **354**, 149–159 (2001).
20. S. Arber, F. A. Barbayannis, H. Hanser, C. Schneider, C. A. Stanyon, O. Bernard, P. Caroni, Regulation of actin dynamics through phosphorylation of cofilin by LIM-kinase. *Nature* **393**, 805–809 (1998).
21. N. Yang, O. Higuchi, K. Ohashi, K. Nagata, A. Wada, K. Kangawa, E. Nishida, K. Mizuno, Cofilin phosphorylation by LIM-kinase 1 and its role in Rac-mediated actin reorganization. *Nature* **393**, 809–812 (1998).
22. D. Pandey, P. Goyal, J. R. Bamburg, W. Siess, Regulation of LIM-kinase 1 and cofilin in thrombin-stimulated platelets. *Blood* **107**, 575–583 (2006).
23. M. Nishita, C. Tomizawa, M. Yamamoto, Y. Horita, K. Ohashi, K. Mizuno, Spatial and temporal regulation of cofilin activity by LIM kinase and Slingshot is critical for directional cell migration. *J. Cell Biol.* **171**, 349–359 (2005).
24. S. Rosso, F. Bollati, M. Bisbal, D. Peretti, T. Sumi, T. Nakamura, S. Quiroga, A. Ferreira, A. Cáceres, LIMK1 regulates Golgi dynamics, traffic of Golgi-derived vesicles, and process extension in primary cultured neurons. *Mol. Biol. Cell* **15**, 3433–3449 (2004).
25. M. Endo, K. Ohashi, K. Mizuno, LIM kinase and Slingshot are critical for neurite extension. *J. Biol. Chem.* **282**, 13692–13702 (2007).
26. S. B. Salvarezza, S. Deborde, R. Schreiner, F. Campagne, M. M. Kessels, B. Qualmann, A. Caceres, G. Kreitzer, E. Rodriguez-Boulan, LIM kinase 1 and cofilin regulate actin filament population required for dynamin-dependent apical carrier fission from the trans-Golgi network. *Mol. Biol. Cell* **20**, 438–451 (2009).
27. V. C. Foletta, N. Moussi, P. D. Sarmiere, J. R. Bamburg, O. Bernard, LIM kinase 1, a key regulator of actin dynamics, is widely expressed in embryonic and adult tissues. *Exp. Cell Res.* **294**, 392–405 (2004).
28. K. Acevedo, N. Moussi, R. Li, P. Soo, O. Bernard, LIM kinase 2 is widely expressed in all tissues. *J. Histochem. Cytochem.* **54**, 487–501 (2006).

29. Y. Meng, Y. Zhang, V. Tregoubov, C. Janus, L. Cruz, M. Jackson, W. Y. Lu, J. F. MacDonald, J. Y. Wang, D. L. Falls, Z. Jia, Abnormal spine morphology and enhanced LTP in LIMK-1 knockout mice. *Neuron* **35**, 121–133 (2002).
30. P. D. Sarmiere, J. R. Bamburg, Head, neck, and spines: A role for LIMK-1 in the hippocampus. *Neuron* **35**, 3–5 (2002).
31. H. Takahashi, U. Koshimizu, J. Miyazaki, T. Nakamura, Impaired spermatogenic ability of testicular germ cells in mice deficient in the LIM-kinase 2 gene. *Dev. Biol.* **241**, 259–272 (2002).
32. Y. Fukazawa, Y. Saitoh, F. Ozawa, Y. Ohta, K. Mizuno, K. Inokuchi, Hippocampal LTP is accompanied by enhanced F-actin content within the dendritic spine that is essential for late LTP maintenance in vivo. *Neuron* **38**, 447–460 (2003).
33. J. Donnerer, R. Schuligoi, C. Stein, Increased content and transport of substance P and calcitonin gene-related peptide in sensory nerves innervating inflamed tissue: Evidence for a regulatory function of nerve growth factor in vivo. *Neuroscience* **49**, 693–698 (1992).
34. C. J. Woolf, B. Safieh-Garabedian, Q. P. Ma, P. Crilly, J. Winter, Nerve growth factor contributes to the generation of inflammatory sensory hypersensitivity. *Neuroscience* **62**, 327–331 (1994).
35. M. Colledge, J. D. Scott, AKAPs: From structure to function. *Trends Cell Biol.* **9**, 216–221 (1999).
36. R. Prekeris, R. M. Hernandez, M. W. Mayhew, M. K. White, D. M. Terrian, Molecular analysis of the interactions between protein kinase C-ε and filamentous actin. *J. Biol. Chem.* **273**, 26790–26798 (1998).
37. M. C. Faux, E. N. Rollins, A. S. Edwards, L. K. Langeberg, A. C. Newton, J. D. Scott, Mechanism of A-kinase-anchoring protein 79 (AKAP79) and protein kinase C interaction. *Biochem. J.* **343**, 443–452 (1999).
38. P. K. Rathee, C. Distler, O. Obreja, W. Neuhuber, G. K. Wang, S. Y. Wang, C. Nau, M. Kress, PKA/AKAP/VR-1 module: A common link of G_s-mediated signaling to thermal hyperalgesia. *J. Neurosci.* **22**, 4740–4745 (2002).
39. I. D. Fraser, M. Cong, J. Kim, E. N. Rollins, Y. Daaka, R. J. Lefkowitz, J. D. Scott, Assembly of an A kinase-anchoring protein–β_2-adrenergic receptor complex facilitates receptor phosphorylation and signaling. *Curr. Biol.* **10**, 409–412 (2000).
40. L. L. Gomez, S. Alam, K. E. Smith, E. Horne, M. L. Dell'Acqua, Regulation of A-kinase anchoring protein 79/150–cAMP-dependent protein kinase postsynaptic targeting by NMDA receptor activation of calcineurin and remodeling of dendritic actin. *J. Neurosci.* **22**, 7027–7044 (2002).
41. G. Bhave, W. Zhu, H. Wang, D. J. Brasier, G. S. Oxford, R. W. Gereau IV, cAMP-dependent protein kinase regulates desensitization of the capsaicin receptor (VR1) by direct phosphorylation. *Neuron* **35**, 721–731 (2002).
42. S. Amadesi, G. S. Cottrell, L. Divino, K. Chapman, E. F. Grady, F. Bautista, R. Karanjia, C. Barajas-Lopez, S. Vanner, N. Vergnolle, N. W. Bunnett, Protease-activated receptor 2 sensitizes TRPV1 by protein kinase Cε- and A-dependent mechanisms in rats and mice. *J. Physiol.* **575**, 555–571 (2006).
43. H. Zhang, C. L. Cang, Y. Kawasaki, L. L. Liang, Y. Q. Zhang, R. R. Ji, Z. Q. Zhao, Neurokinin-1 receptor enhances TRPV1 activity in primary sensory neurons via PKCε: A novel pathway for heat hyperalgesia. *J. Neurosci.* **27**, 12067–12077 (2007).
44. Z. Y. Zhuang, H. Xu, D. E. Clapham, R. R. Ji, Phosphatidylinositol 3-kinase activates ERK in primary sensory neurons and mediates inflammatory heat hyperalgesia through TRPV1 sensitization. *J. Neurosci.* **24**, 8300–8309 (2004).
45. C. Morenilla-Palao, R. Planells-Cases, N. García-Sanz, A. Ferrer-Montiel, Regulated exocytosis contributes to protein kinase C potentiation of vanilloid receptor activity. *J. Biol. Chem.* **279**, 25665–25672 (2004).
46. Y. R. Yang, Y. He, Y. Zhang, Y. Li, Y. Li, Y. Han, H. Zhu, Y. Wang, Activation of cyclin-dependent kinase 5 (Cdk5) in primary sensory and dorsal horn neurons by peripheral inflammation contributes to heat hyperalgesia. *Pain* **127**, 109–120 (2007).
47. T. Sumi, K. Matsumoto, Y. Takai, T. Nakamura, Cofilin phosphorylation and actin cytoskeletal dynamics regulated by Rho- and Cdc42-activated LIM-kinase 2. *J. Cell Biol.* **147**, 1519–1532 (1999).
48. K. Mizuno, Signaling mechanisms and functional roles of cofilin phosphorylation and dephosphorylation. *Cell. Signal.* **25**, 457–469 (2013).
49. R. Niwa, K. Nagata-Ohashi, M. Takeichi, K. Mizuno, T. Uemura, Control of actin reorganization by Slingshot, a family of phosphatases that dephosphorylate ADF/cofilin. *Cell* **108**, 233–246 (2002).
50. Y. Ohta, K. Kousaka, K. Nagata-Ohashi, K. Ohashi, A. Muramoto, Y. Shima, R. Niwa, T. Uemura, K. Mizuno, Differential activities, subcellular distribution and tissue expression patterns of three members of Slingshot family phosphatases that dephosphorylate cofilin. *Genes Cells* **8**, 811–824 (2003).
51. M. J. Caterina, A. Leffler, A. B. Malmberg, W. J. Martin, J. Trafton, K. R. Petersen-Zeitz, M. Koltzenburg, A. I. Basbaum, D. Julius, Impaired nociception and pain sensation in mice lacking the capsaicin receptor. *Science* **288**, 306–313 (2000).
52. J. B. Davis, J. Gray, M. J. Gunthorpe, J. P. Hatcher, P. T. Davey, P. Overend, M. H. Harries, J. Latcham, C. Clapham, K. Atkinson, S. A. Hughes, K. Rance, E. Grau, A. J. Harper, P. L. Pugh, D. C. Rogers, S. Bingham, A. Randall, S. A. Sheardown, Vanilloid receptor-1 is essential for inflammatory thermal hyperalgesia. *Nature* **405**, 183–187 (2000).
53. L. Yu, F. Yang, H. Luo, F. Y. Liu, J. S. Han, G. G. Xing, Y. Wan, The role of TRPV1 in different subtypes of dorsal root ganglion neurons in rat chronic inflammatory nociception induced by complete Freund's adjuvant. *Mol. Pain* **4**, 61 (2008).
54. R. R. Ji, T. A. Samad, S. X. Jin, R. Schmoll, C. J. Woolf, p38 MAPK activation by NGF in primary sensory neurons after inflammation increases TRPV1 levels and maintains heat hyperalgesia. *Neuron* **36**, 57–68 (2002).
55. P. Cesare, P. McNaughton, A novel heat-activated current in nociceptive neurons and its sensitization by bradykinin. *Proc. Natl. Acad. Sci. U.S.A.* **93**, 15435–15439 (1996).
56. X. Zhang, L. Li, P. A. McNaughton, Proinflammatory mediators modulate the heat-activated ion channel TRPV1 via the scaffolding protein AKAP79/150. *Neuron* **59**, 450–461 (2008).
57. K. E. Brandao, M. L. Dell'Acqua, S. R. Levinson, A-kinase anchoring protein 150 expression in a specific subset of TRPV1- and $Ca_V1.2$-positive nociceptive rat dorsal root ganglion neurons. *J. Comp. Neurol.* **520**, 81–99 (2012).
58. K. Schnizler, L. P. Shutov, M. J. Van Kanegan, M. A. Merrill, B. Nichols, G. S. McKnight, S. Strack, J. W. Hell, Y. M. Usachev, Protein kinase A anchoring via AKAP150 is essential for TRPV1 modulation by forskolin and prostaglandin E_2 in mouse sensory neurons. *J. Neurosci.* **28**, 4904–4917 (2008).
59. N. A. Jeske, A. M. Patwardhan, N. B. Ruparel, A. N. Akopian, M. S. Shapiro, M. A. Henry, A-kinase anchoring protein 150 controls protein kinase C-mediated phosphorylation and sensitization of TRPV1. *Pain* **146**, 301–307 (2009).
60. M. J. Fischer, J. Btesh, P. A. McNaughton, Disrupting sensitization of transient receptor potential vanilloid subtype 1 inhibits inflammatory hyperalgesia. *J. Neurosci.* **33**, 7407–7414 (2013).
61. M. Shinoda, M. Asano, D. Omagari, K. Honda, S. Hitomi, A. Katagiri, K. Iwata, Nerve growth factor contribution via transient receptor potential vanilloid 1 to ectopic orofacial pain. *J. Neurosci.* **31**, 7145–7155 (2011).
62. F. F. Hefti, A. Rosenthal, P. A. Walicke, S. Wyatt, G. Vergara, D. L. Shelton, A. M. Davies, Novel class of pain drugs based on antagonism of NGF. *Trends Pharmacol. Sci.* **27**, 85–91 (2006).
63. E. J. Huang, L. F. Reichardt, Trk receptors: roles in neuronal signal transduction. *Annu. Rev. Biochem.* **72**, 609–642 (2003).
64. D. C. Edwards, G. N. Gill, Structural features of LIM kinase that control effects on the actin cytoskeleton. *J. Biol. Chem.* **274**, 11352–11361 (1999).
65. M. Kobayashi, M. Nishita, T. Mishima, K. Ohashi, K. Mizuno, MAPKAPK-2-mediated LIM-kinase activation is critical for VEGF-induced actin remodeling and cell migration. *EMBO J.* **25**, 713–726 (2006).
66. R. R. Ji, R. W. Gereau IV, M. Malcangio, G. R. Strichartz, MAP kinase and pain. *Brain Res. Rev.* **60**, 135–148 (2009).
67. C. A. Pritchard, L. Hayes, L. Wojnowski, A. Zimmer, R. M. Marais, J. C. Norman, B-Raf acts via the ROCKII/LIMK/cofilin pathway to maintain actin stress fibers in fibroblasts. *Mol. Cell. Biol.* **24**, 5937–5952 (2004).
68. C. Hough, F. Fukamauchi, D. M. Chuang, Regulation of β-adrenergic receptor mRNA in rat C_6 glioma cells is sensitive to the state of microtubule assembly. *J. Neurochem.* **62**, 421–430 (1994).
69. C. Keenan, D. Kelleher, Protein kinase C and the cytoskeleton. *Cell. Signal.* **10**, 225–232 (1998).
70. S. Ahn, S. Maudsley, L. M. Luttrell, R. J. Lefkowitz, Y. Daaka, Src-mediated tyrosine phosphorylation of dynamin is required for β_2-adrenergic receptor internalization and mitogen-activated protein kinase signaling. *J. Biol. Chem.* **274**, 1185–1188 (1999).
71. T. T. Cao, H. W. Deacon, D. Reczek, A. Bretscher, M. von Zastrow, A kinase-regulated PDZ-domain interaction controls endocytic sorting of the β2-adrenergic receptor. *Nature* **401**, 286–290 (1999).
72. Y. G. Wang, A. M. Samarel, S. L. Lipsius, Laminin binding to β_1-integrins selectively alters β_1- and β_2-adrenoceptor signalling in cat atrial myocytes. *J. Physiol.* **527**, 3–9 (2000).
73. R. L. Rivard, M. Birger, K. J. Gaston, A. K. Howe, AKAP-independent localization of type-II protein kinase A to dynamic actin microspikes. *Cell Motil. Cytoskeleton* **66**, 693–709 (2009).
74. R. V. Størkson, A. Kjørsvik, A. Tjølsen, K. Hole, Lumbar catheterization of the spinal subarachnoid space in the rat. *J. Neurosci. Methods* **65**, 167–172 (1996).
75. B. M. Xing, Y. R. Yang, J. X. Du, H. J. Chen, C. Qi, Z. H. Huang, Y. Zhang, Y. Wang, Cyclin-dependent kinase 5 controls TRPV1 membrane trafficking and the heat sensitivity of nociceptors through KIF13B. *J. Neurosci.* **32**, 14709–14721 (2012).

Funding: This work was supported by grants from the National Natural Science Foundation of China (91332119, 81161120497, 30925015, and 30830044 to Y.W.; 31371143 and 30900582 to Y.Z.; 81221002 to L.L.; and 30800330 to J.W.), a grant (973 Program: 2014CB542204 to Y.W.) from the Ministry of Science and Technology of China, the Beijing Natural Science Foundation (7132130 to J.W.), and an open project of the Key Laboratory of Mental Health, Institute of Psychology, Chinese Academy of Sciences. **Author contributions:** Y.W., J.W., and Y.L. designed the experiments; Y.L., F.H., H.-J.C., Y.-J.D., and Z.-Y.X. performed the experiments; and Y.W., J.W., and Y.Z. wrote the paper. **Competing interests:** The authors declare that they have no competing interests.

Submitted 9 April 2014
Accepted 6 June 2014
Final Publication 24 June 2014
10.1126/scisignal.2005353
Citation: Y. Li, F. Hu, H.-J. Chen, Y.-J. Du, Z.-Y. Xie, Y. Zhang, J. Wang, Y. Wang, LIMK-dependent actin polymerization in primary sensory neurons promotes the development of inflammatory heat hyperalgesia in rats. *Sci. Signal.* **7**, ra61 (2014).